

Phosphorylation of the RNase III enzyme Drosha at Serine300 or Serine302 is required for its nuclear localization

Xiaoli Tang, Yingjie Zhang, Lynne Tucker and Bharat Ramratnam*

Laboratory of Retrovirology, Division of Infectious Diseases, Department of Medicine, Warren Alpert Medical School of Brown University, Providence, RI 02903, USA

Received January 29, 2010; Revised May 27, 2010; Accepted May 28, 2010

ABSTRACT

The RNase III enzyme Drosha plays a pivotal role in microRNA (miRNA) biogenesis by cleaving primary miRNA transcripts to generate precursor miRNA in the nucleus. The RNA binding and enzymatic domains of Drosha have been characterized and are on its C-terminus. Its N-terminus harbors a nuclear localization signal. Using a series of truncated Drosha constructs, we narrowed down the segment responsible for nuclear translocation to a domain between aa 270 and aa 390. We further identified two phosphorylation sites at Serine300 (S300) and Serine302 (S302) by mass spectrometric analysis. Double mutations of S→A at S300 and S302 completely disrupted nuclear localization. Single mutation of S→A at S300 or S302, however, had no effect on nuclear localization indicating that phosphorylation at either site is sufficient to locate Drosha to the nucleus. Furthermore, mimicking phosphorylation status by mutating S→E at S300 and/or S→D at S302 restored nuclear localization. Our findings add a further layer of complexity to the molecular anatomy of Drosha as it relates to miRNA biogenesis.

INTRODUCTION

MicroRNAs (miRNAs) are a class of endogenous non-protein-coding small RNAs of ~22 nt in length that impact gene expression by sequence-specific interaction with homologous mRNA (1). Presently, it is thought that miRNAs most commonly repress gene expression by base-pairing with the 3'-untranslated region (UTR) of their target mRNAs. However, recent work has also identified miRNA that target coding sequences of genes (2). Additionally, miRNA may also target promoter

regions and thereby act as pro-transcriptional elements, as in the case of miRNA-373 and the gene encoding E-cadherin (3). One specific miRNA may inhibit many target genes and one specific gene may be regulated by more than one miRNA. For example, both miRNA-125a and b, the genes of which are located on different chromosomes, target the p53 protein as both miRNAs harbor similar seed sequences that share similarity to the p53 3'UTR (4,5). MiRNAs play increasingly recognized roles in several basic processes including cell signal transduction, tumorigenesis, tumor invasion and metastasis, stem cell renewal, immune function, apoptosis and reaction to stress (6–11). The vast majority of miRNA genes are thought to be under the control of RNAP II with others being recently identified as substrates of RNAP III (12,13). Irrespectively, miRNA genes are initially transcribed to yield a primary, long transcript that undergoes successive processing in both the nucleus and cytoplasm. Nuclear processing is mediated by the RNase III enzyme Drosha–DGCR8 (DiGeorge Syndrome Critical Region Gene 8) microprocessor complex to generate precursor miRNAs (pre-miRNAs) of ~70 nt in length. Pre-miRNAs are subsequently transported to the cytoplasm by export 5-Ran-GTP where they are cleaved by the RNase III enzyme Dicer to generate mature miRNAs (14–18).

Investigation into the molecular mechanisms of miRNA biogenesis at the transcriptional and translational levels has been intensively pursued (19–22). Drosha plays a central role in miRNA biogenesis and recent work suggests that its expression level directly influences clinical outcomes in malignant disease thus underlying the importance of better understanding mechanisms that impact Drosha expression and function (23). Along these lines, Drosha has been found to interact with other host proteins including DGCR8. Drosha and DGCR8 regulate each other post-transcriptionally. The Drosha–DGCR8 complex destabilizes DGCR8 mRNA by cleaving its hairpin structure. DGCR8, in turn, stabilizes Drosha via

*To whom correspondence should be addressed. Tel: +1 401 444 5219; Fax: +1 401 444 2939; Email: bramratnam@lifespan.org

protein–protein interaction (22). In an elegant experiment, deletion of Drosha N-terminal 390 amino acids had no effect on its binding with DGCR8 and its ability to process pri-miRNA *in vitro* (21). While these results suggested that the N-terminal region is dispensable *vis-a-vis* the protein's catalytic activity, they also raised an interesting question: what role, if any, does N-terminal sequence play in Drosha function *in vivo*?

Here, we examine the subcellular localization of wild-type Drosha and N-terminally deleted Drosha. We find that wild-type Drosha locates to the nucleus, as expected, but Drosha with N-terminal 390 amino acids deleted is located exclusively in the cytoplasm. These results were in agreement with previous work which found that the N-terminus of Drosha is not dispensable but rather essential for its nuclear localization and ultimate miRNA processing function (24). We further narrowed down the domain for nuclear localization to the N-terminal region between aa 270 and aa 390. We show by microscopy and functional assays that phosphorylation at Serine300 or Serine302 is absolutely required for the nuclear localization and subsequent miRNA processing activities of Drosha.

MATERIALS AND METHODS

Plasmids and primers

pcDNA4/TO/cmcyDrosha was originally created by Thomas Tuschl and deposited at Addgene (Addgene plasmid 10828; 25). Wild-type and mutated Drosha were subcloned into pEGFP-C1 vector (GenBank Accession #:U55763) using restriction endonucleases HindIII and KpnI (New England Biolabs cat.# R0104L and cat.#R0142L, respectively). Point mutants were generated with site-directed mutagenesis techniques as previously described (26). The primers used for PCR were ordered from Integrated DNA Technologies. The primer sequences are shown in Supplementary Table S1. psiCHECK2-miRNA-143 plasmid was created by inserting antisense target sequences of miRNA-143 ds-oligos (sense:CCGCTCGAGGAGCTATAGTGCTTCATCTCAGCGGCCGAAAAGGAAAA and antisense: TTTTCCTTTTGCGGCCGCTGAGATGAAGCACTATAGCTCCTCGAGCGG) into psiCHECK2 vector (Promega) using NotI and XhoI (New England Biolabs) restriction endonuclease sites. All the cDNA constructs were verified by DNA sequencing at Yale KECK Foundation Biotechnology Resource Laboratory.

Antibodies and reagents

Anti-RNase III Drosha (H-300) rabbit polyclonal antibody (sc-33778), Anti-IkB-a (C-21) rabbit polyclonal antibody (sc-371), anti-Lamin A (H-102) rabbit polyclonal antibody (sc-20680), anti-GFP (B-2) mouse monoclonal antibody (sc-9996) and Protein G Plus-Agarose (sc-2002) were purchased from Santa Cruz Biotechnology. Pfu DNA Polymerase (cat.#600136) and dNTP mix (cat.#200415-51) were purchased from Stratagene. Lipofectamine Reagent (cat.#18324-020) and Lipofectamine 2000 Reagent (cat.#11668-019) were

purchased from Invitrogen. Alexa Fluor 680 goat anti-rabbit IgG (H&L) (cat.#A21076) and Hoechst 33342 (cat.#H3570) were purchased from Invitrogen Molecular Probes. IRDye800-conjugated Affinity Purified Anti-Mouse IgG (H&L) (cat.#610-132-121) was purchased from Rockland Immunochemicals. Tris-Glycine-SDS Running Buffer (cat.#BP-150) and Transfer Buffer (cat.#BP-190) were purchased from Boston Bioproducts. LB Agar Kanamycin-50 Plates (cat.#L0643) and EDTA (cat.#E7889) were purchased from Sigma. The 10×Tris-Buffered Saline (cat.#170-6435) and 10% Tween20 solution (cat.#161-0781) were purchased from Bio-Rad Laboratories. Complete Mini, EDTA-free Protease Inhibitor Cocktail Tablets (cat.#11 836 170 001) was produced by Roche Diagnostics GmbH. QIAprep Spin Miniprep Kit (cat.#27106), QIAquick PCR Purification Kit (cat.#28106) and MinElute Gel Extraction Kit (cat.#28604) were purchased from QIAGEN. Coomassie Brilliant Blue R-250 Dye (cat.#20278) was purchased from Thermo Scientific.

Cell culture and transfection

HEK293T and Huh-7 cells were cultured in Dulbecco's modified Eagle's medium (Invitrogen, Carlsbad, CA, USA) with 10% fetal bovine serum and 2 mM L-glutamine. HeLa cells were grown in Eagle's Minimum Essential Medium supplemented with 10% fetal bovine serum, 2 mM L-glutamine and non-essential amino acids. Cells were trypsinized and reseeded in culture plates 1 day before transfection. HEK293T transfection was performed with Lipofectamine when cell confluency was ~60%. Huh-7 and HeLa cells were transfected with Lipofectamine 2000 when cell confluency was ~80%.

Cytoplasmic and nuclear fractionation

Cytoplasmic and nuclear fractionation was performed using EZ Nuclei Isolation Kit (Sigma, cat.#NUC-101) according to the manufacturer's instructions. Briefly, cells were harvested and washed once with cold PBS. The cells were then suspended in EZ Nuclei Isolation buffer and rotated at 4°C for 5 min. After centrifugation at 4°C for 5 min, supernatant was collected containing the cytoplasmic fraction. Cell lysis and centrifugation were repeated three times. The final pellets were collected as the nuclear fraction and lysed in modified RIPA buffer (50 mM Tris-HCl pH 7.4, 150 mM NaCl, 2 mM EDTA, 1% NP-40, 1% Triton X-100).

Western blotting

Cell lysates (100 µg protein each) were separated by 10% SDS-PAGE electrophoresis and electroblotted to nitrocellulose membrane (Bio-Rad, cat.#162-0115). Blotted membranes were probed with their respective primary antibodies rotating at 4°C overnight. The membranes were washed three times in TBST buffer and probed with secondary antibody (Alexa Fluor 680 goat anti-rabbit IgG or IRDye800-conjugated Affinity Purified Anti-Mouse IgG, respectively) at room temperature for 1 h. Membranes were then washed three times in TBST buffer and direct infrared fluorescence detection

was performed with a Licor Odyssey[®] Infrared Imaging System (26).

LC-MS/MS mass spectrometry analysis of protein with post-translational modifications

HEK293T cells were transfected with 20 µg cDNA of GFP-Drosha. Two milligrams of protein lysate was incubated with 5 µg anti-GFP monoclonal antibody at 4°C for 1 h. Protein G Plus-Agarose beads (80 µl) were added into the lysate. The lysate-antibody-bead mixture was rotated at 4°C overnight. The immunoprecipitated beads were subsequently washed three times with RIPA buffer, resolved by 10% SDS-PAGE and visualized using Coomassie blue staining. The GFP-Drosha protein band was excised and subjected to mass spectrometric analysis performed by the Taplin Biological Mass Spectrometry Facility (Boston, MA, USA; 26).

Confocal fluorescent imaging

HEK293T, Huh-7 or HeLa cells were transfected with constructs expressing GFP or GFP-tagged wild-type or mutated Drosha, respectively. Twenty-four hours post-transfection, the cells were trypsinized and reseeded at 1:10 dilution. The cells were incubated for another 24 h. Hoechst 33342 (final concentration 1 µg/ml) was added to cell culture 30 min before confocal fluorescent imaging which was performed with a LeicaTCS SP2 AOBS confocal laser microscope.

Cell sorting and real-time PCR

HEK293T cells were transfected with constructs expressing GFP alone (as EV control) or GFP-tagged wild-type or mutated Drosha, respectively. Twenty-four hours post-transfection, the cells were trypsinized and resuspended in a sort buffer (1 × Ca/Mg⁺⁺-free phosphate buffered saline, 1 mM EDTA, 25 mM HEPES pH 7.0, 1% heat-inactivated fetal bovine serum, 10 µ/ml DNase I). GFP-positive cells were sorted out with FACSVantage SE (Becton Dickinson) to respective collection tubes. The collected cells were used for RNA extraction. Total RNA was extracted by TRIZOL (Invitrogen) and 1 µg of total RNA was used for cDNA synthesis using MMLV reverse transcriptase (New England Biolabs). TaqMan[®] microRNA assay (Applied Biosystems) that include RT primers and TaqMan probes was used to quantify the levels of mature miRNA and 18S RNA was used for normalization. All PCR reactions were run in triplicate.

Luciferase assays

We used the psi-CHECK2 system (Promega) to create sensor assays for quantifying mature miRNA-143 function by placing the anti-sense sequence of miRNA-143 in the 3'UTR of the gene encoding *Renilla* luciferase. In the presence of mature miRNA-143, the luciferase activity of *Renilla* decreases through the classical RNAi pathway. HEK 293T cells were co-transfected with psiCHECK2, pcDNA3miR-143 (a RNAP II promoter driven miRNA-143 expression vector) and

Drosha expression constructs or empty vector. Firefly and *Renilla* luciferase activities were quantified using the Dual-Luciferase Reporter Assay System (Promega) and *Renilla* luciferase activity was normalized to firefly luciferase activity. For each experiment, a control employing an empty vector was used and corrected luciferase values were averaged, arbitrarily set to a value of '1' and served as a reference for comparison of fold-differences in experimental values.

Northern blot

A miRNA-143 expression plasmid and Drosha wt or mutant constructs were transfected into HEK293T cells using lipofectamine reagent. Forty-eight hour post-transfection, total RNA was prepared with Trizol reagent. Twenty micrograms of total RNA was used for northern blotting analysis following conventional protocols but using a biotin-labeled probe and BrightStar BioDetect[™] Nonisotopic Detection Kit (Ambion).

Statistical/Bioinformatics analysis

The Drosha protein sequence was mined for potential phosphorylation sites using the PredictProtein program (<http://www.predictprotein.org>). Mixed linear models (proc mixed, SAS version 9.2, SAS Institute, Cary, NC, USA) were used for statistical analysis as described previously (27).

RESULTS

GFP-tagged Drosha locates in the nucleus

We first quantified Drosha expression in a number of human cell lines including HEK293T, Huh-7 and HeLa cells by cytoplasmic and nuclear fractionation followed by western blot analysis. As expected, our data (Figure 1A, top panel) revealed that Drosha exclusively localized to the nuclei of the tested cells. Cytoplasmic marker IkBa and nuclear marker Lamin A were used as controls to confirm the stringency of our nuclear isolation methods (Figure 1A, middle panel and bottom panel, respectively). We then subcloned Drosha into pEGFP-C1 vector to generate the reporter construct GFP-Drosha. Importantly, sequences encoding GFP do not harbor a nuclear localization signal (NLS) or a nuclear export signal (NES). As expected, introduction of the parental GFP construct into HEK293T cells led to diffuse GFP expression (Figure 1B, top panel). In contrast, introduction of GFP-Drosha was associated with exclusive GFP expression in the nuclei of HEK293T cells (Figure 1B, bottom panel). We repeated these experiments in other human cell lines such as HeLa (Supplementary Figure S1) and Huh-7 and obtained exactly similar results. These experiments suggested that sequences encoding Drosha harbored a putative NLS that was not affected by the addition of sequence encoding GFP.

The N-terminus of Drosha harbors a NLS

As GFP-Drosha was exclusively expressed in the nucleus, we reasoned that there must be a strong NLS in Drosha.

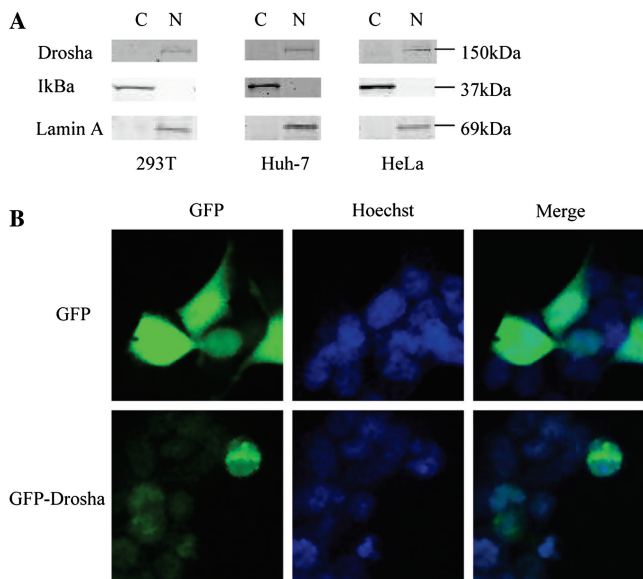


Figure 1. Droscha localizes to the nucleus. (A) Endogenous Droscha protein was detected in the nuclei of HEK293T, Huh-7 and HeLa cells by western blot analysis. Cells were harvested when 100% confluent. Cytoplasmic and nuclear fractionation was performed. IκBα and Lamin A served as cytoplasmic and nuclear markers, respectively (C, cytoplasmic; N, nuclear). (B) Overexpression of a construct encoding Droscha tagged with GFP on the N-terminus localizes to the nucleus. HEK293T cells were transfected with GFP backbone vector alone or GFP-tagged Droscha plasmid, respectively. Hoechst 33342 was used to stain the nuclei 30 min before fluorescent imaging was performed. Top panel: GFP backbone vector expression showing diffuse localization. Bottom panel: GFP-Droscha expression showing nuclear localization.

To pinpoint its location, we constructed a series of GFP-Droscha deletion constructs as illustrated in Figure 2A. A construct in which the C-terminal 524 amino acids was deleted (Droscha Δ C524) localized exclusively to the nucleus (Figure 2B, top panel). In contrast, when we deleted the entire N-terminus (aa 1–390), Droscha localized exclusively to the cytoplasm (Figure 2B, upper middle panel) providing a general location for its NLS. We then focused on better defining the molecular anatomy of the N-terminus which localizes to the nucleus exclusively (Figure 2B, down middle panel). We deleted N-terminal 217 amino acids and a corresponding reporter construct GFP-Droscha Δ N217 still localized to the nucleus exclusively (Figure 2B, bottom panel). All these results were confirmed in other cell lines including Huh-7 and HeLa cells (Supplementary Figure S1).

A domain between aa 270 and aa 390 of Droscha harbors a NLS

In silico screening of the Droscha protein sequence predicted two potential NLSs: NLS1 (243-RHRSLDRRER-252) and NLS2 (276-RHRSYERSRERERERHRHR-295). We constructed GFP-Droscha reporter constructs with either NLS1 or NLS2 or both being deleted (Figure 3A). GFP-Droscha_{270–1374} with NLS1 deleted localized to the nucleus (Figure 3B, top panel) indicating that this predicted NLS1 site is not essential for correct

cellular localization. We next focused on the NLS2 site. Surprisingly, we encountered similar results in that the NLS2 deleted variant also localized to the nucleus (Figure 3B, middle panel). Lastly, a reporter construct GFP-Droscha_{270–1374} Δ NLS2 in which both NLS1 and NLS2 were deleted also localized to the nucleus (Figure 3B, bottom panel) clearly suggesting that a nuclear localization mechanism distinct from the canonical NLS in the domain between aa 270 and aa 390 of Droscha is operational.

Identification of phosphorylation sites by mass spectrometry analysis

Protein phosphorylation plays an important role in nuclear localization (28,29). For example, phosphorylation of extracellular signal-regulated kinase (ERK)-2 at Ser244 and Ser246 induced its nuclear translocation. Additionally, phosphorylation of β -catenin at Ser191 and Ser605 controls its nuclear localization. We next asked if Droscha is constitutively phosphorylated and whether phosphorylation status impacts nuclear localization. The cell lysate from HEK293T cells transfected with GFP-Droscha for 48 h without any treatment was immunoprecipitated with anti-GFP mouse monoclonal antibody and Protein G Plus-Agarose beads. The precipitate was resolved by SDS-PAGE and stained with Coomassie Brilliant Blue R-250 Dye. The gel showed a clear band corresponding to the calculated size of GFP-Droscha (Figure 4A). This band was excised and subjected to LC-MS/MS mass spectrometry. The results confirmed that the excised band was indeed purified GFP-Droscha with two phosphorylation sites at Serine300 and Serine302 being identified (Figure 4B).

Phosphorylation at Serine300 or Serine302 locates Droscha to the nucleus

Based upon the MS results, we made a series of GFP-Droscha constructs with different point mutations involving the putative phosphorylation sites as indicated. Single S \rightarrow A mutation at S300 or S302 did not change the nuclear localization of GFP-Droscha (Figure 5A and B, respectively). Double mutations at S300 and S302, however, totally prevented nuclear localization producing a cellular staining pattern similar to GFP without NLS (Figure 5C). These results indicated that S300 and S302 were constitutively phosphorylated and that phosphorylation at either site was sufficient to locate Droscha to the nucleus. This was further supported by mutating Serine300 to glutamic acid (E), and Serine302 to aspartic acid (D). Indeed, all of these phosphorylation mimics (GFP-Droscha_{S300E}, GFP-Droscha_{S302D} and GFP-Droscha_{S300E/S302D}) located Droscha in the nuclei of HEK293T cells (Figure 5D–F). Again, these results were reproducible in other cell lines including HeLa cells (Supplementary Figures S1 and S2).

Nuclear localization of Droscha is critical for its functionality in miRNA processing

The fact that Droscha is indispensable for cellular health posed a challenge for assigning a critical *in vivo* function to

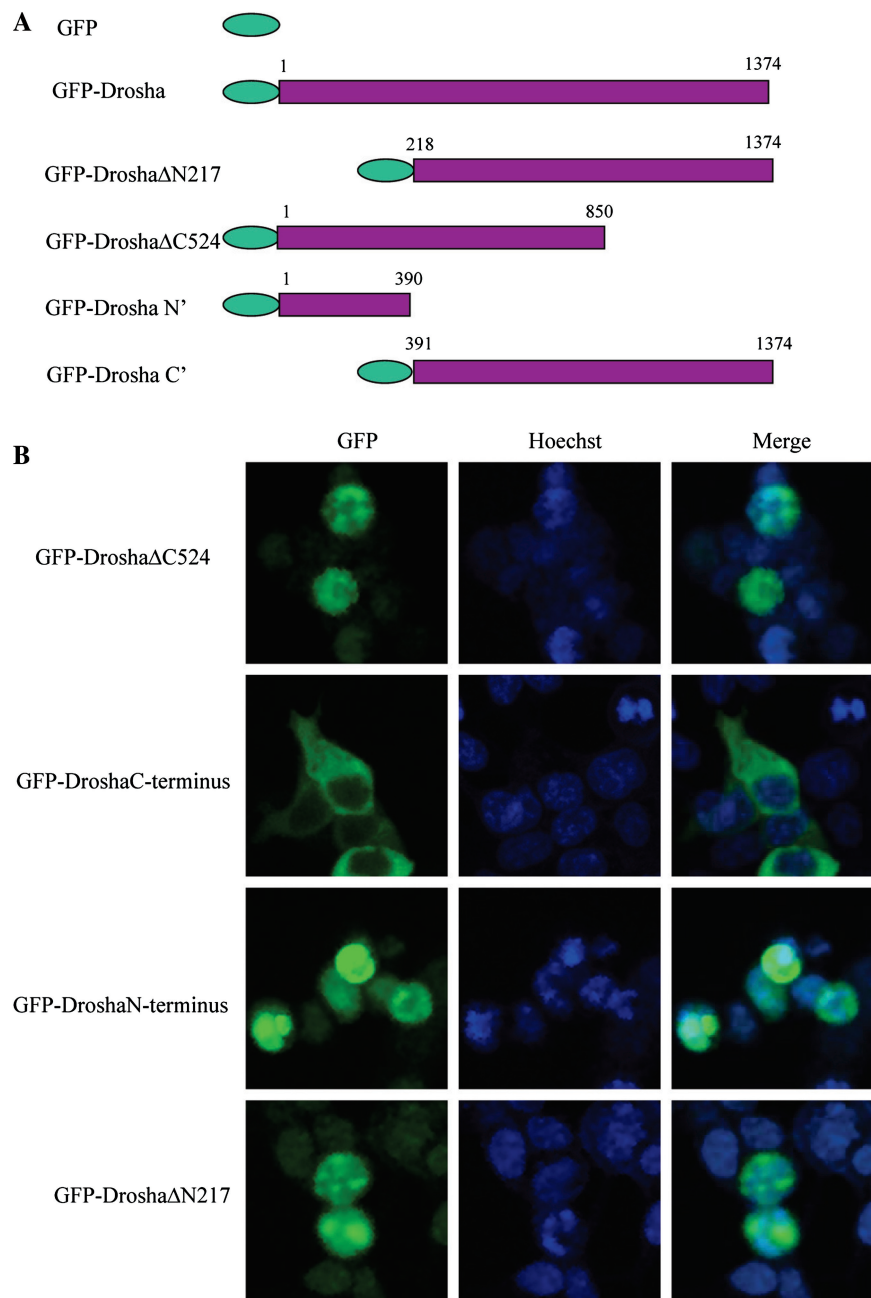


Figure 2. The N-terminus of Drosha is critical for nuclear localization. **(A)** Schematic illustration of domain deletion constructs of Drosha tagged with GFP at the N-terminus. **(B)** Cellular localization of different Drosha deletion mutants. Top panel: nuclear localization of GFP–Drosha with C-terminal 524 amino acid deletion. Upper middle panel: cytoplasmic localization of GFP–Drosha C-terminus. Lower middle panel: nuclear localization of GFP–Drosha N-terminus. Bottom panel: nuclear localization of GFP–Drosha with N-terminal 217 amino acid deletion.

the N-terminus using our various constructs. The purest experiment, after all, would be to use a Drosha null cell and introduce our various constructs as well as miRNA expression cassettes to examine their downstream effect on miRNA processing. To our knowledge, no Drosha null human cell line exists. We therefore relied upon ectopic expression of both our various Drosha constructs as well as miRNA expression cassettes. We first confirmed that all our Drosha constructs produced similar levels of protein upon cellular transfection, thereby removing the possibility that differential protein expression of our constructs

was the ultimate effector of miRNA processing activity (Figure 6A). As previously reported, HEK293T cells harbor relatively low levels of mature miRNA-143 (27). Interestingly, these cells also express relatively low levels of endogenous Drosha when compared to other cell lines such as HCT116, NIH3T3, etc. Accordingly, we transfected cells with the GFP vector alone (empty vector), GFP–Drosha WT or the various GFP–Drosha mutated constructs along with an expression plasmid encoding miRNA-143. FACS was used to obtain GFP expressing cells. Real-time PCR was performed to measure

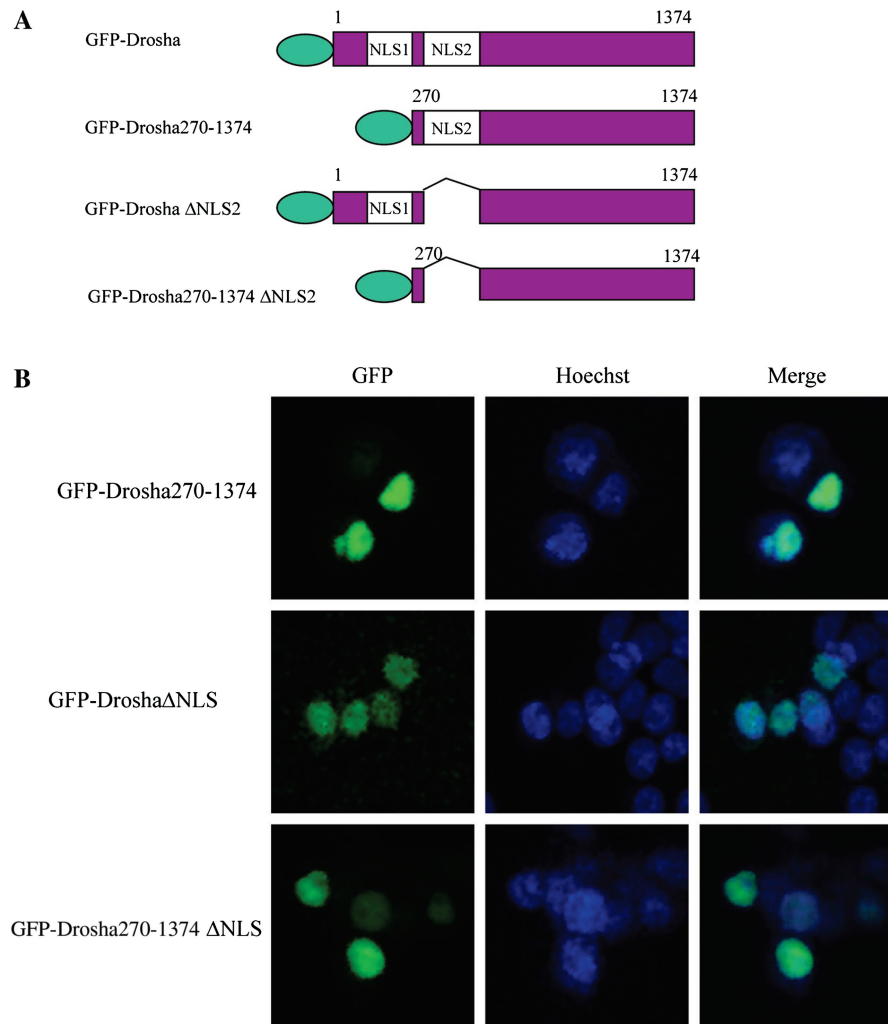


Figure 3. The domain for nuclear localization. **(A)** Schematic illustration of domain deletion constructs of Drosha tagged with GFP at the N-terminus. **(B)** Cellular localization of different Drosha deletion mutants. Top panel: nuclear localization of GFP–Drosha with N-terminal 269 amino acid deletion. Middle panel: nuclear localization of GFP–Drosha with NLS2 deletion. Bottom panel: nuclear localization of GFP–Drosha with N-terminal 269 amino acid and NLS2 deletion.

miRNA-143 and northern blot was performed to identify pre- and mature miRNA-143 species. Our data revealed that overexpression of GFP–Drosha WT, S300A, S302A, S300E, S302D or S300E/S302D led to the production of pre- and mature miRNA-143 (Figure 6B and D). However, cells expressing GFP–DroshaS300/302A or GFP–Drosha C-terminus (aa 391–1374) did not retain the ability to produce mature or pre-miRNA-143. These results were further validated by miRNA sensor assays. For example, co-transfection of the sensor along with GFP–Drosha led to a statistically significant reduction in *Renilla* activity compared to empty vector. GFP–DroshaS300A, S302A, S300E, S302D or S300E/S302D behaved similarly to GFP–Drosha. In contrast, cellular introduction of GFP–DroshaS300/302A had no significant effect on sensor activity compared to empty vector (Figure 6C). We then repeated this experiment but used sensors for miRNA-26b and 125a. Again, similar results were encountered with the stereotypical loss of miRNA activity in transfections involving only

GFP–DroshaS300/302A or GFP–Drosha C-terminus (aa 391–1374; Supplementary Figure S3). Lastly, we further reasoned that these nonfunctional Drosha mutants should impede the processing of pri-miRNA and thereby lead to an accumulation of this species. Indeed, real-time PCR quantification of pri-miRNA-143 revealed a 2-fold increase in experiments involving the cytoplasmic localized Drosha variants [GFP–DroshaS300/302A or GFP–Drosha C-terminus (aa 391–1374)] compared to bonafide nuclear localized variants (Supplementary Figure S4).

DISCUSSION

A myriad of proteins exist in a single cell and their correct subcellular localization is critical for protein function and cellular health. The RNaseIII enzyme Drosha is a nuclear protein and correct localization is essential to its function in processing pri-miRNA species in the canonical pathway of miRNA biogenesis. The nuclear transporting

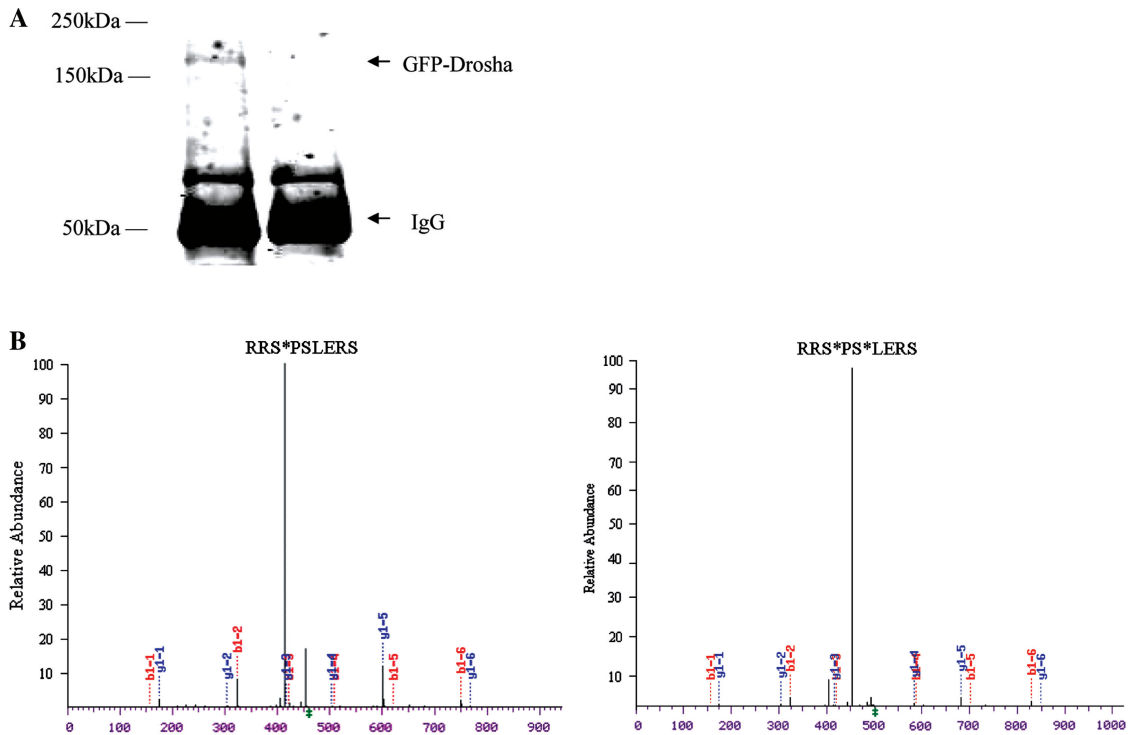


Figure 4. Identification of phosphorylation sites by mass spectrometry. (A) Immunoprecipitation of GFP-Drosha with anti-GFP monoclonal antibody. HEK293T cells were transfected with a GFP-Drosha construct (or empty vector as a control) using Lipofectamine. Whole-cell lysate was prepared with modified RIPA buffer 48 h post-transfection and resultant immunoprecipitants were submitted for MS analysis (lane 1, GFP-Drosha; lane 2, a transfection with an irrelevant construct as a negative control). (B) Identification of phosphorylation sites by mass spectrometry. The Coomassie stained GFP-Drosha protein band was excised and mass spectrometry analysis was performed. The asterisk shows the phosphorylated serine.

mechanisms involving Drosha are unknown. Given the central role of miRNA in many basic cellular processes, any factor that adversely affects the nuclear location of Drosha is likely to disturb miRNA biogenesis and eventually influence the normal function of the cell.

Most nuclear proteins use a NLS to target themselves to the nucleus. Typical NLS consist of an amino acid sequence with positively charged lysines or arginines (30). *In silico* screening predicted two potential NLS (NLS1 and NLS2) on Drosha. To determine if NLS1 and NLS2 were functional for Drosha, we generated a series of wild-type and mutant Drosha constructs with GFP tagged to the N-termini to monitor the protein localization. GFP is a widely used reporter protein that does not change the function and subcellular location when added as a protein tag (31,32). Furthermore, GFP does not harbor a NLS or a nuclear export signal (NES), thereby accounting for its diffuse expression upon cellular introduction. GFP-Drosha and GFP-Drosha1-390 localized to the nucleus. However, GFP-Drosha391-1374 exclusively localized to the cytoplasm. These results raised the possibility that the C-terminus of Drosha might contain a NES which perhaps was inhibited by a strong NLS in the full-length context. Deletion of the N-terminus may have exposed this NES or abolished its inhibition.

In silico analysis revealed the presence of two putative NLS sites in the N-terminus of Drosha.

GFP-Drosha270-1374 with deletion of NLS1 located in the nucleus. GFP-Drosha270-1374 Δ NLS2 with deletion of both NLS1 and NLS2 still located in the nucleus indicating that both NLS1 and NLS2 were dispensable for the nuclear localization of Drosha. This prompted us to hypothesize that Drosha might use a nuclear localization mechanism other than the canonical NLS to locate to the nucleus. In reality, the canonical NLS motif is absent in many proteins that localize to the nucleus. Proteins without canonical NLS may contain Serine-Proline-Serine (SPS) motif. Phosphorylation at either serine can facilitate binding with nuclear transporter (28). This prompted us to identify putative phosphorylation sites in the N-terminus of Drosha. A series of reporter constructs revealed that phosphorylation at Serine 300 or Serine 302 is critical for Drosha nuclear localization. A phosphorylated SPS motif acting as a NLS was initially found in signal proteins such as ERKs, Smad3 and MEK1 (28). Our results suggest that Drosha may use a similar pathway for correct nuclear localization. We note that phosphorylation at either or both serine sites could change the conformation of Drosha and thereby alter its affinity for putative binding partners. Further investigation is clearly warranted to identify proteins that interact with Drosha on the SPS motif as this motif appears highly conserved among mammals (Supplementary Figure S5).

Reversible phosphorylation of proteins is an important regulatory mechanism in which kinases (phosphorylation)

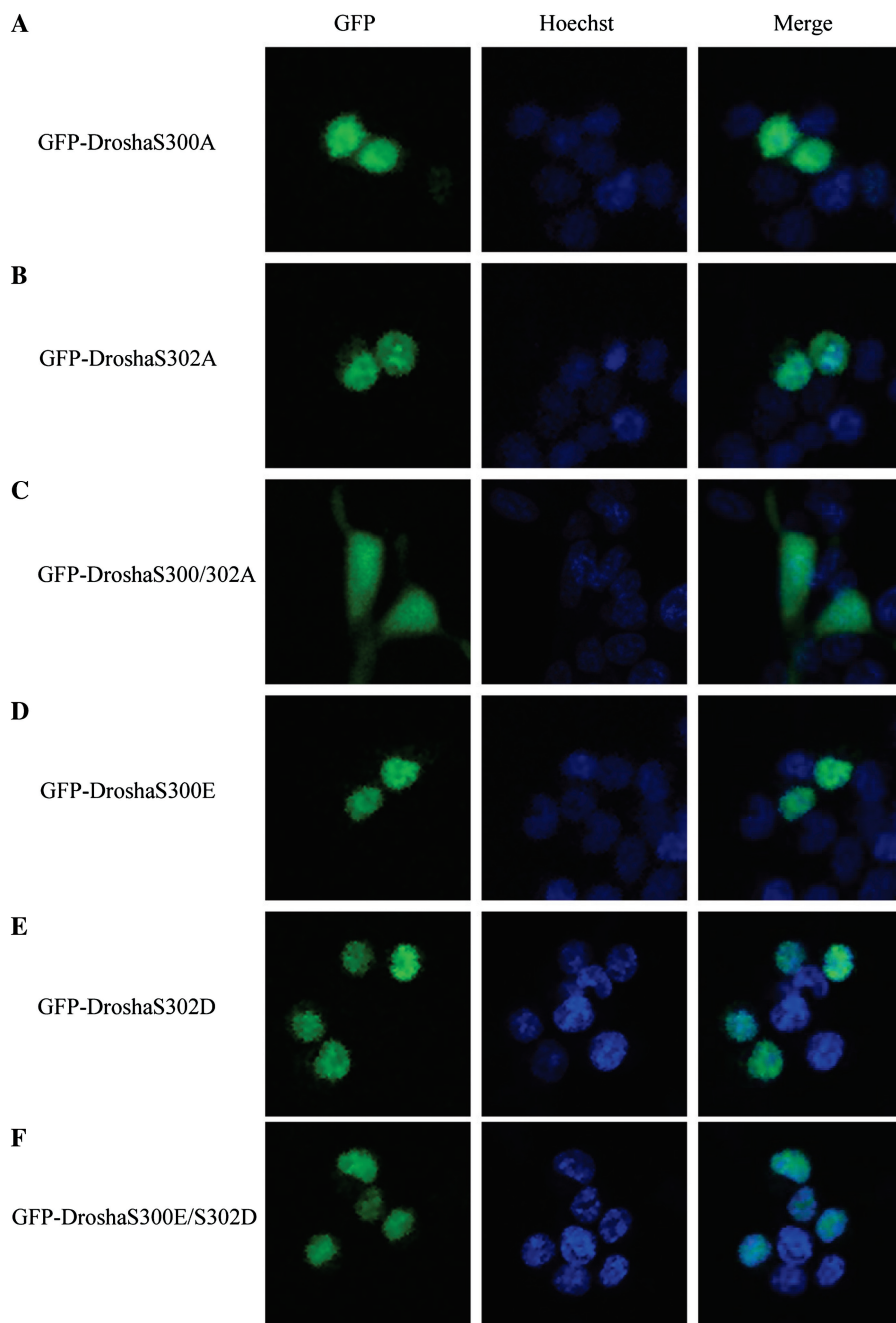


Figure 5. Phosphorylation at S300 or S302 locates Drosha to the nucleus. Experimental procedures were the same as in Figure 1B but used different constructs as indicated. (A) Expression of GFP–Drosha with Serine300 mutated to Alanine showing nuclear localization. (B) Expression of GFP–Drosha with Serine302 mutated to Alanine also showed nuclear localization. (C) Expression of GFP–Drosha with both serines mutated to alanines showing diffuse cellular localization similar to that of GFP without NLS. (D) Expression of GFP–Drosha with Serine300 mutated to glutamic acid showed nuclear localization. (E) Expression of GFP–Drosha with Serine302 mutated to aspartic acid showing nuclear localization. (F) Expression of GFP–Drosha with Serine300 mutated to glutamic acid and Serine302 mutated to aspartic acid also showed nuclear localization.

and phosphatases (dephosphorylation) are involved. Phosphorylation plays critical roles in signal transduction, protein localization and degradation (33–35). We have consistently identified Drosha phosphorylation at S300 and S302 from immunoprecipitated endogenous and overexpressed Drosha by mass spectrometry analysis. The potential kinases which phosphorylate S300 and S302 could include cyclin dependent kinase

(CDK)5, glycogen synthase kinase(GSK)3, mitogen activated protein kinase(MAPK)3, MAPK2, MAPK8, protein kinase A(PKA), protein kinase C α (PKC α), protein kinase B(PKB), casein kinaseI (*CKI*), etc. All of our data indicate that these serine sites might be constitutively phosphorylated by multiple kinases. Identification of the specific enzymes which affect Drosha phosphorylation status may reveal new insights into miRNA

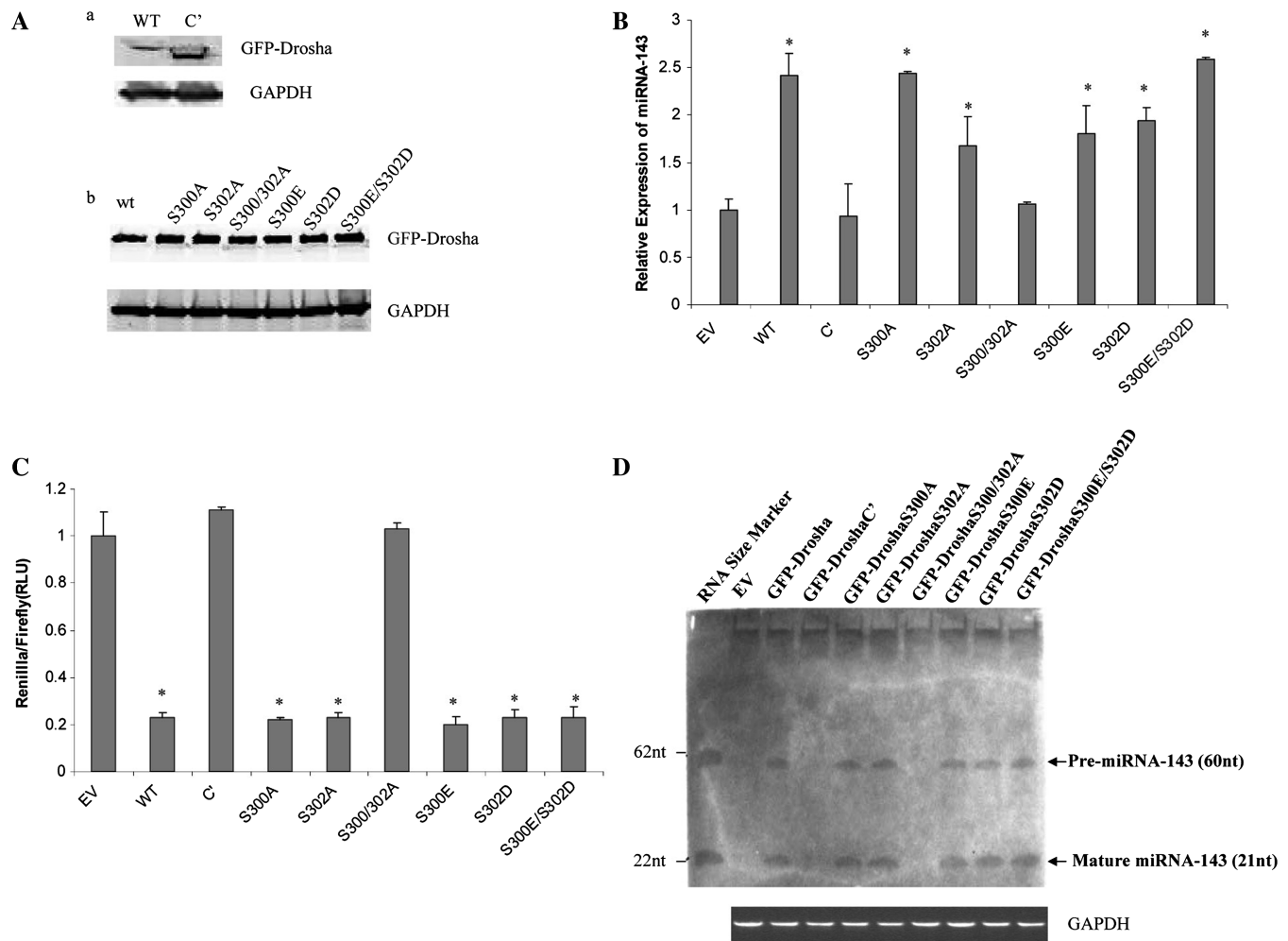


Figure 6. Nuclear localization of Drosha is critical for its functionality in miRNA processing. (A) Protein expression levels of wt Drosha and mutants. GFP-tagged Drosha wt or mutant constructs were transfected into HEK293T cells using lipofectamine reagent. Forty-eight hours post-transfection, protein lysates were prepared from the transfected cells and protein levels were measured by western blot analysis. GAPDH was used as a loading control. All constructs produced equivalent levels of Drosha protein. (B) Quantification of mature miRNA-143 levels/function by real-time PCR (B), miRNA sensor assays (C) and northern blot (D). GFP vector alone (empty vector, EV), GFP-Drosha wide type (WT) or different mutant constructs as indicated were transfected into HEK 293T cells along with a miRNA-143 expression vector. Twenty-four hours post-transfection, GFP-positive cells were cell sorted for RNA extraction. Endogenous mature miRNA-143 level was quantified by using a specific miRNA-143 Taqman real-time PCR kit. All experiments were performed in triplicate (compared to EV, $*P < 0.05$). (C) miRNA sensor assays revealed that compared to EV control conditions, cells that had been transfected with Drosha constructs that localized to the cytoplasm (GFP-DroshaC' and GFP-DroshaS300/302A) were associated with impaired miRNA function. All experiments were performed in triplicate (compared to EV, $*P < 0.05$). (D). Effects of overexpressed Drosha wt or mutants on miRNA-143 biogenesis by northern blotting analysis. Cells transfected with cytoplasmic Drosha localized constructs did not retain the ability to process pri-miRNA-143 with the absence of pre- and mature species in GFP-DroshaC' and GFP-DroshaS300/302A treated cells.

deregulation that is seen in diverse disease states including cancer.

SUPPLEMENTARY DATA

Supplementary Data are available at NAR Online.

ACKNOWLEDGEMENTS

We thank Ross Tomaino for help in mass spectrometry analysis, Ginny Hovanesian for assistance in fluorescent imaging, Sara Spangenberg for assistance in cell sorting

and Jin Song Gao for technical support in performing the miRNA sensor assays.

FUNDING

National Institutes of Health (P20RR025179 and R01AI058697); Lifespan/Brown/Tufts CFAR (P30AI042853); National Institutes of Health (number T32DA013911 to X.T.). Funding for open access charge: National Institutes of Health.

Conflict of interest statement. None declared.

REFERENCES

1. Lee, R.C., Feinbaum, R.L. and Ambros, V. (1993) The *C. elegans* heterochronic gene *lin-4* encodes small RNAs with antisense complementarity to *lin-14*. *Cell*, **75**, 843–854.
2. Tay, Y., Zhang, J., Thomson, A.M., Lim, B. and Rigoutsos, I. (2008) MicroRNAs to *Nanog*, *Oct4* and *Sox2* coding regions modulate embryonic stem cell differentiation. *Nature*, **455**, 1124–1128.
3. Place, R.F., Li, L.C., Pookot, D., Noonan, E.J. and Dahiya, R. (2008) MicroRNA-373 induces expression of genes with complementary promoter sequences. *Proc. Natl Acad. Sci. USA*, **105**, 1608–1613.
4. Zhang, Y., Gao, J.S., Tang, X., Tucker, L.D., Quesenberry, P., Rigoutsos, I. and Ramratnam, B. (2009) MicroRNA 125a and its regulation of the p53 tumor suppressor gene. *FEBS Lett.*, **583**, 3725–3730.
5. Le, M.T., Teh, C., Shyh-Chang, N., Xie, H., Zhou, B., Korzh, V., Lodish, H.F. and Lim, B. (2009) MicroRNA-125b is a novel negative regulator of p53. *Genes Dev.*, **23**, 862–876.
6. John, B., Enright, A.J., Aravin, A., Tuschl, T., Sander, C. and Marks, D.S. (2004) Human microRNA targets. *PLoS Biol.*, **2**, e363.
7. Zhang, W., Dahlberg, J.E. and Tam, W. (2007) MicroRNAs in tumorigenesis: a primer. *Am. J. Pathol.*, **171**, 728–738.
8. Gregory, R.I. and Shiekhattar, R. (2005) MicroRNA biogenesis and cancer. *Cancer Res.*, **65**, 3509–3512.
9. Ma, L., Teruya-Feldstein, J. and Weinberg, R.A. (2007) Tumour invasion and metastasis initiated by microRNA-10b in breast cancer. *Nature*, **449**, 682–688.
10. Garzon, R., Fabbri, M., Cimmino, A., Calin, G.A. and Croce, C.M. (2006) MicroRNA expression and function in cancer. *Trends Mol. Med.*, **12**, 580–587.
11. Leung, A.K. and Sharp, P.A. (2007) microRNAs: a safeguard against turmoil? *Cell*, **130**, 581–585.
12. Lee, Y., Kim, M., Han, J., Yeom, K.H., Lee, S., Baek, S.H. and Kim, V.N. (2004) MicroRNA genes are transcribed by RNA polymerase II. *EMBO J.*, **23**, 4051–4060.
13. Borchert, G.M., Lanier, W. and Davidson, B.L. (2006) RNA polymerase III transcribes human microRNAs. *Nat. Struct. Mol. Biol.*, **13**, 1097–1101.
14. Lee, Y., Ahn, C., Han, J., Choi, H., Kim, J., Yim, J., Lee, J., Provost, P., Rådmark, O., Kim, S. *et al.* (2003) The nuclear RNase III Droscha initiates microRNA processing. *Nature*, **425**, 415–419.
15. Landthaler, M., Yalcin, A. and Tuschl, T. (2004) The human DiGeorge syndrome critical region gene 8 and its D. melanogaster homolog are required for miRNA biogenesis. *Curr. Biol.*, **14**, 2162–2167.
16. Winter, J., Jung, S., Keller, S., Gregory, R.I. and Diederichs, S. (2009) Many roads to maturity: microRNA biogenesis pathways and their regulation. *Nat. Cell Biol.*, **11**, 228–234.
17. Han, J., Lee, Y., Yeom, K.H., Nam, J.W., Heo, I., Rhee, J.K., Sohn, S.Y., Cho, Y., Zhang, B.T. and Kim, V.N. (2006) Molecular basis for the recognition of primary microRNAs by the Droscha-DGCR8 complex. *Cell*, **125**, 887–901.
18. Kim, V.N., Han, J. and Siomi, M.C. (2009) Biogenesis of small RNAs in animals. *Nat. Rev. Mol. Cell Biol.*, **10**, 126–139.
19. Zeng, Y. and Cullen, B.R. (2005) Efficient processing of primary microRNA hairpins by Droscha requires flanking nonstructured RNA sequences. *J. Biol. Chem.*, **280**, 27595–27603.
20. Nilsen, T.W. (2007) Mechanisms of microRNA-mediated gene regulation in animal cells. *Trends Genet.*, **23**, 243–249.
21. Han, J., Lee, Y., Yeom, K.H., Kim, Y.K., Jin, H. and Kim, V.N. (2004) The Droscha-DGCR8 complex in primary microRNA processing. *Genes Dev.*, **18**, 3016–3027.
22. Han, J., Pedersen, J.S., Kwon, S.C., Belair, C.D., Kim, Y.K., Yeom, K.H., Yang, W.Y., Harssler, D., Belloch, R. and Kim, V.N. (2004) Posttranscriptional crossregulation between Droscha and DGCR8. *Cell*, **136**, 75–84.
23. Merritt, W.M., Lin, Y.G., Han, L.Y., Kamat, A.A., Spannuth, W.A., Schmandt, R., Urbauer, D., Pennacchio, L.A., Cheng, J.F., Nick, A.M. *et al.* (2008) Dicer, Droscha, and outcomes in patients with ovarian cancer. *N. Engl. J. Med.*, **359**, 2641–2650.
24. Lee, Y., Han, J., Yeom, K.H., Jin, H. and Kim, V.N. (2006) Droscha in primary microRNA processing. *Cold Spring Harb. Symp. Quant. Biol.*, **71**, 51–57.
25. Landthaler, M., Yalcin, A. and Tuschl, T. (2004) The human DiGeorge syndrome critical region gene 8 and its D. melanogaster homolog are required for miRNA biogenesis. *Curr. Biol.*, **14**, 2162–2167.
26. Tang, X., Gao, J.S., Guan, Y.J., McLane, K.E., Yuan, Z.L., Ramratnam, B. and Chin, Y.E. (2007) Acetylation-dependent signal transduction for type I interferon receptor. *Cell*, **131**, 93–105.
27. Gao, J.S., Zhang, Y., Li, M., Tucker, L.D., Machan, J.T., Quesenberry, P., Rigoutsos, I. and Ramratnam, B. (2010) Atypical transcription of microRNA gene fragments. *Nucleic Acids Res.*, **38**, 2775–2787.
28. Chuderland, D., Konson, A. and Seger, R. (2008) Identification and characterization of a general nuclear translocation signal in signaling proteins. *Mol. Cell*, **31**, 850–861.
29. Wu, X., Tu, X., Joeng, K.S., Hilton, M.J., Williams, D.A. and Long, F. (2008) Rac1 activation controls nuclear localization of beta-catenin during canonical Wnt signaling. *Cell*, **133**, 340–353.
30. Kalderon, D., Roberts, B.L., Richardson, W.D. and Smith, A.E. (1984) A short amino acid sequence able to specify nuclear location. *Cell*, **39**, 499–509.
31. Tsien, R.Y. (1998) The green fluorescent protein. *Annu. Rev. Biochem.*, **67**, 509–544.
32. Lin, M.Z., Glenn, J.S. and Tsien, R.Y. (2008) A drug-controllable tag for visualizing newly synthesized proteins in cells and whole animals. *Proc. Natl Acad. Sci. USA*, **105**, 7744–7749.
33. Gong, X., Tang, X., Wiedmann, M., Wang, X., Peng, J., Zheng, D., Blair, L.A., Marshall, J. and Mao, Z. (2003) Cdk5-mediated inhibition of the protective effects of transcription factor MEF2 in neurotoxicity-induced apoptosis. *Neuron*, **38**, 33–46.
34. Tang, X., Wang, X., Gong, X., Tong, M., Park, D., Xia, Z. and Mao, Z. (2005) Cyclin-dependent kinase 5 mediates neurotoxin-induced degradation of the transcription factor myocyte enhancer factor 2. *J. Neurosci.*, **25**, 4823–4834.
35. Vervoorts, J., Lüscher-Firzlaff, J. and Lüscher, B. (2006) The ins and outs of MYC regulation by posttranslational mechanisms. *J. Biol. Chem.*, **281**, 34725–34729.